Received: 4 December 2018 | Revised: 25 February 2019 | Accepted: 1 April 2019

DOI: 10.1002/asl.900

Atmospheric Science Letters RMetS

RESEARCH ARTICLE

Tropical precipitation influencing boreal winter midlatitude blocking

Gereon Gollan[1] | **Swantje Bastin**[1] | **Richard J. Greatbatch**[1,2]

[1]Ocean Circulation and Climate Dynamics, GEOMAR Helmholtz Centre for Ocean Research Kiel, Kiel, Germany

[2]Faculty of Mathematics and Natural Sciences, Kiel University, Kiel, Germany

Correspondence
Gereon Gollan, Ocean Circulation and Climate Dynamics, GEOMAR Helmholtz Centre for Ocean Research Kiel, Kiel D-24105, Germany.
Email: ggollan@geomar.de

Recent studies using reanalysis data and complex models suggest that the Tropics influence midlatitude blocking. Here, the influence of tropical precipitation anomalies is investigated further using a dry dynamical model driven by specified diabatic heating anomalies. The model uses a quasi-realistic setup based on idealized orography and an idealized representation of the land-ocean thermal contrast. Results concerning the El Niño Southern Oscillation and the Madden-Julian Oscillation are mostly consistent with previous studies and emphasize the importance of tropical dynamics for driving the variability of blocking at midlatitudes. It is also shown that a common bias in models of the Coupled Model Intercomparison Project Phase 5 (CMIP5), namely, excessive tropical precipitation, leads to an underestimation of midlatitude blocking in our model, also a common bias in the CMIP5 models. The strongest blocking anomalies associated with the tropical precipitation bias are found over Europe, where the underestimation of blocking in CMIP5 models is also particularly strong.

KEYWORDS

blocking bias, CMIP5, dry atmospheric general circulation model, ENSO, Midlatitude blocking, MJO, precipitation bias

1 | INTRODUCTION

Boreal winter midlatitude blocking (MLB) is one of the major large-scale atmospheric circulation patterns, which is characterized by a diversion of the midlatitude jet stream and the embedded storm systems by a persistent high-pressure anomaly. MLB is associated with important impacts on surface temperature and precipitation, for example, leading to sometimes persistent cold spells or dry periods. A correct representation of MLB should therefore be a priority for model development, to allow for a useful prediction of blocking on synoptic to climatic time scales. However, almost all atmospheric models—from all generations of models, no matter if coupled to the ocean or not—have serious problems in simulating the correct location and frequency of MLB (Masato *et al.,* 2013; Davini and D'Andrea, 2016). The problem is especially evident over the eastern North Atlantic (NA) and Europe, where most models show a negative bias in MLB frequency. Biases in MLB in the models can severely reduce seasonal forecast skill over Europe and also decrease confidence in the regional patterns of projected climate change. The negative bias in MLB frequency can be reduced, for example, by increasing model resolution (Scaife *et al.,* 2011; Jung *et al.,* 2012; Berckmans *et al.,* 2013), improving the representation of orography and tuning the convective parametrization (Jung *et al.,* 2010). These improvements in MLB result at least partly from improvements in the mean circulation at midlatitudes (Scaife *et al.,* 2011; Berckmans *et al.,* 2013), which is biased in most models. In terms of the mean state, the position and the

strength of the jet stream—and the jet exit regions in particular—appear essential for a correct simulation of the climatology of MLB.

The variability of MLB has been shown to be influenced by tropical variability. For example, the positive (negative) phase of El Niño Southern Oscillation (ENSO) is associated with reduced (increased) blocking over the midlatitude North Pacific (NP) (Renwick and Wallace, 1996; Barriopedro *et al.,* 2006). Over the NA and European sector, results are less clear in reanalyses, and previous studies suggest only a weak ENSO influence in general (Henderson and Maloney, 2018) or slightly reduced high-latitude blocking (HLB) over the NA during La Niña (Gollan and Greatbatch, 2017). Also, those phases of the Madden–Julian Oscillation (MJO, Wheeler and Hendon, 2004) characterized by enhanced convection over the Maritime Continent and the western tropical Pacific, are associated with enhanced blocking over the NA and Europe (e.g., Cassou, 2008; Gollan *et al.,* 2015; Henderson *et al.,* 2016). The mechanism by which ENSO and the MJO influence the extratropics is mainly by diabatic heating anomalies associated with upper-level divergence leading to Rossby wave source anomalies in regions of a strong subtropical jet (e.g., Sardeshmukh and Hoskins, 1988). The representation of the above teleconnections is therefore partly dependent on the location and strength of the diabatic heating anomalies associated with ENSO or the MJO, another source of uncertainty in models (Hinton *et al.,* 2009). The other main source of uncertainty is, as pointed out above, biases in the extratropical mean flow that can change the characteristics of the subtropical jet and, thus, the generation and propagation of Rossby waves.

Here, we use a dynamical core of an atmosphere-only model with idealized orography and idealized land-ocean temperature contrasts to yield an estimate of the steady-state extratropical response to tropical diabatic heating anomalies (Section 2.1). Experiments driven by diabatic heating anomalies resembling precipitation anomalies associated with ENSO and the MJO will enhance confidence in results obtained from reanalysis data and other models. Furthermore, we test the hypothesis that a positive bias in tropical precipitation, which is common to numerous models, leads to the biased MLB frequency in the models.

2 | METHODS

2.1 | Model and experimental setup

The Portable University Model of the Atmosphere (PUMA, Fraedrich *et al.,* 1998) is a dry dynamical core model based on the multilevel spectral model described by Hoskins and Simmons (1975). The model is run with triangular spectral truncation at wavenumber 42 (T42, roughly corresponding to 312-km resolution) in the horizontal and 30 sigma levels up to 10^{-4} hPa in the vertical. Friction and diabatic heating are represented linearly by Rayleigh friction and Newtonian cooling, respectively. As proposed by Held and Suarez (1994), we use a zonally symmetric, meridionally sinusoidal restoration temperature distribution in the troposphere as the basic setup, with a temperature difference of 20 K between the South and the North Pole (i.e., boreal winter), while the stratosphere is relaxed to a constant temperature of 200 K (i.e., no statospheric polar vortex is included). All experiments use a basic setup with two Gaussian-shaped mountain ranges of 6,000 m height, one representing the Rocky Mountains and one representing the Himalayas. Furthermore, two temperature dipoles are added to the background temperature in the middle troposphere, which are Gaussian-shaped in all three dimensions, mimicking the land-ocean temperature contrasts at the eastern coasts of North America and of Eurasia, respectively, separated by 160° in longitude. Note that Franzke *et al*. (2000) used the same model (PUMA) with similar heating dipoles, but without including orography, and found the most realistic storm tracks using a zonal separation of 150° of the heating dipoles. For a detailed description of the model parameters, the reader is referred to Supporting Information (Text S1, Figure S1) and to Bastin (2018). In the following, we use a 264-year reference run with the basic setup described above to calculate anomalies for the sensitivity experiments. The blocking climatology (see Section 2.2 for the blocking index used here) of the reference run is remarkably similar to a December–January–February (DJF) climatology obtained from reanalysis data, while noting that the modeled blocking frequency is only about half of the observed frequency and that the blocking peaks are slightly shifted to the east compared to observations (see Figure S2 and the green contours in Figure 1). The relatively low blocking frequencies in the model compared to reanalysis might be related to the fact that there is no stratospheric polar vortex in our model that could provide dynamical feedback (see Woollings *et al.,* 2010).

To revisit the results of previous studies on the MLB response to ENSO and the MJO using reanalysis data, we perform sensitivity experiments adding diabatic heating anomalies to the PUMA model at the Equator. The diabatic heating anomalies are Gaussian-shaped in all three dimensions (see Supporting Information for exact specifications) and are designed to resemble the precipitation anomalies associated with the different phases of ENSO and the MJO. Diabatic heating amplitudes of 1.0 K day^{-1} and 1.5 K day^{-1} in the middle troposphere are used that correspond to moderate MJO and weak ENSO events, respectively (see Morita *et al.,* 2006). Note that the ENSO forcing used here is only a monopole heating, whereas in reality there is rather a dipole heating (e.g., for El Niño, there is anomalous heating over the eastern tropical Pacific and anomalous cooling over the Maritime Continent). Hinton *et al*. (2009) found that the opposing heating centers associated with ENSO can have

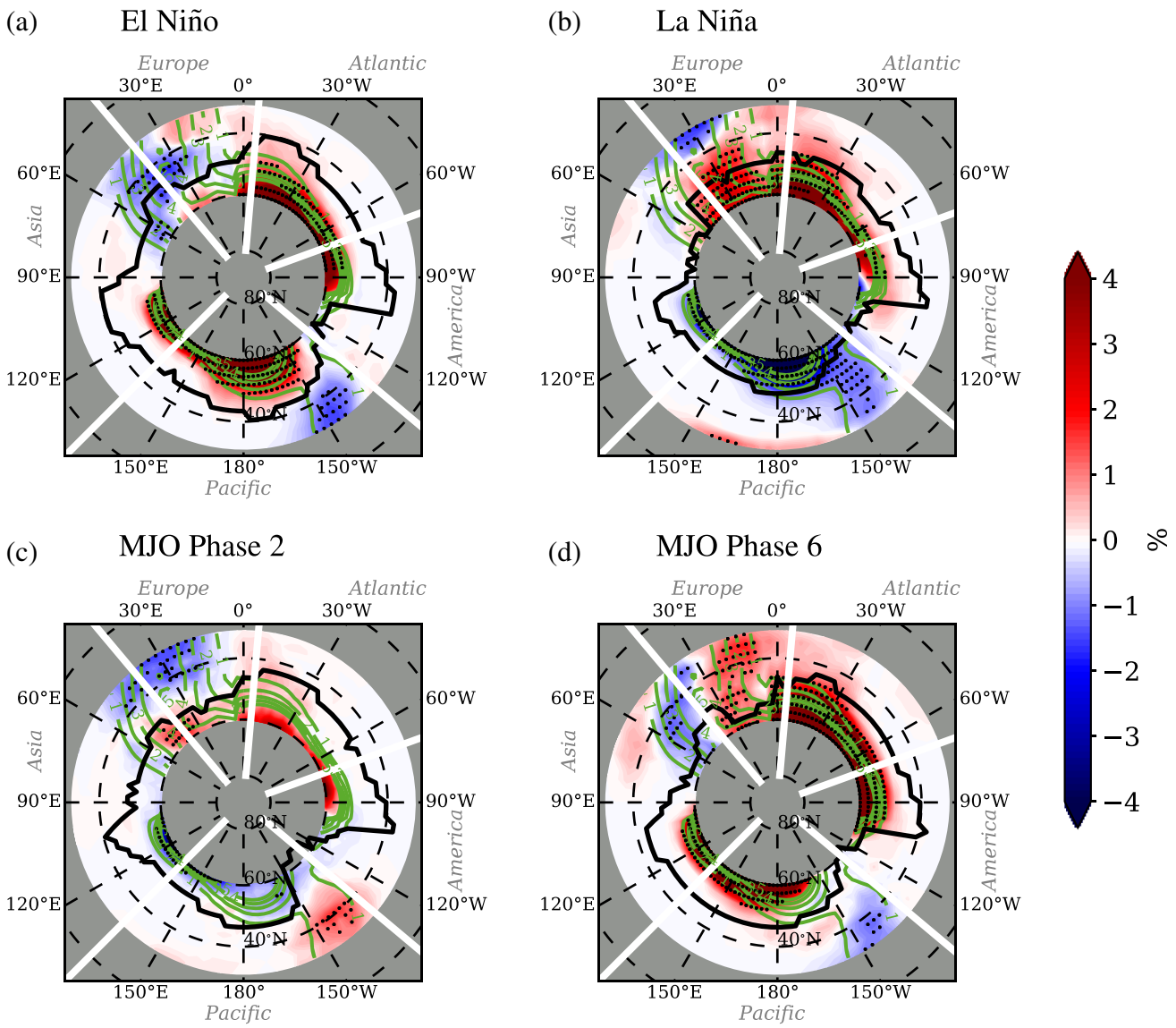

FIGURE 1 Polar stereographic projection of the two-dimensional blocking frequency anomalies for the (a, b) ENSO and (c, d) MJO sensitivity experiments with respect to the climatology of the reference experiment. The climatology of the reference experiment is shown as labeled green contours (1% contour interval). Black dots show statistical significance of the blocking anomalies at the 95% level (see Supporting Information for details). Black solid line shows the climatological position of the storm track (see Methods for details). Gray is overlaid where no blocking index has been computed. White solid lines separate five different sectors of the Northern Hemisphere, which are indicated on the outside of the boxes (Europe, Atlantic, America, Pacific, and Asia)

opposing effects on NP blocking, motivating us to use monopole heating. Therefore, a direct comparison with results from reanalysis might be misleading. The sensitivity to the amplitude of the diabatic heating anomalies was previously tested with different magnitudes (see Bastin, 2018), and the response was found to increase approximately linearly with amplitude in most cases. All sensitivity experiments are run for 22 years and the first two years of integration are discarded as spin-up. Note that the background restoration temperature corresponds to boreal winter (DJF) during the whole integration, that is, there is no seasonal cycle in our experiments.

2.2 | Analysis methods

Similar to the absolute geopotential height index defined by Scherrer *et al.* (2006), the two-dimensional instantaneous blocking index is defined here as

$$BI_{\text{inst}}(\lambda,\phi)=\frac{1}{\Delta\phi}\int_{\phi}^{\phi+\Delta\phi}Z(\lambda,\phi')d\phi'-\frac{1}{\Delta\phi}\int_{\phi-\Delta\phi}^{\phi}Z(\lambda,\phi')d\phi', \tag{1}$$

where λ denotes the longitude, ϕ latitude, $Z(\lambda, \phi)$ is the geopotential height at the location (λ, ϕ) and $\Delta\phi = 15^{\circ}$. Note

that Z at 300 hPa is used here instead of the usual 500-hPa level to avoid intersection with the mountains in the model. However, the results in the following are not qualitatively sensitive to this choice. The above definition of BI_{inst} measures the meridional gradient of Z that is usually negative in the Northern Hemisphere. An actual blocking event is then detected if BI_{inst} is positive, meaning reversed, for at least 4 days and over at least 15° longitude (similar to previous studies, for example, Gollan *et al.,* 2015; Gollan and Greatbatch, 2017).

For further analyses of our model experiments, storm tracks are identified using the power spectral density (PSD) of Z at 300 hPa integrated over periods of 2–6 days. The maximum of Northern Hemisphere PSD at each longitude then defines the latitude of the storm track.

3 | RESULTS

3.1 | MLB response to tropical heating associated with ENSO and the MJO

In Figure 1a and b, the blocking frequency anomalies with respect to the reference run are shown for the ENSO experiment, while in Figure 2 the geopotential height anomalies and storm track anomalies are shown. While blocking frequency anomalies at latitudes higher than 60°N often reach absolute values larger than 15%, we use a color range of ±4% here to focus on MLB. It is evident in Figure 1a that for the El Niño experiment there is enhanced (reduced) MLB frequency north (south) of the climatological storm track in the Pacific sector. The time mean geopotential height (Z) over the NP (see Figure 2a) shows a reduced meridional gradient north of 50°N, consistent with enhanced blocking there. The storm track at midlatitudes is strengthened (Figure 2c), consistent with reduced MLB over the eastern NP. In the La Niña experiment, there is a wide reduction in MLB frequency over the NP (Figure 1b), connected to a northward shift of the storm track (Figure 2d). There is also a weakened meridional gradient in geopotential height (Z) at subtropical latitudes over the central NP during La Niña (Figure 2b), consistent with the hint of enhanced blocking there. Over the western NA, HLB is enhanced for both El Niño and La Niña conditions, suggesting a nonlinear teleconnection to the NA sector. The increase in MLB for La Niña is likely to be related to a weakened NA storm track compared to the reference run (see Figure 2d), while the NA storm track for El Niño is strengthened, but shifted to the south by about 5° also consistent with enhanced blocking at mid to high latitudes. Over continental Europe, there is a decrease (increase) in MLB frequency for El Niño (La Niña), related to a strengthened (weakened) storm track there.

The results for ENSO agree well with Gollan and Greatbatch (2017) over the Pacific, who found similar MLB anomalies in reanalysis data and in a seasonal forecasting model. Over the western NA, the increase of HLB frequency for both El Niño and La Niña is contrary to Gollan and Greatbatch (2017) and also to Henderson and Maloney (2018) who both find a weak decrease in HLB frequency for both cases. Over midlatitude Europe, results agree qualitatively with the model results of Gollan and Greatbatch (2017), who find a weak decrease (increase) in MLB frequency for El Niño (La Niña). Note again that there is no stratospheric polar vortex in the model used here, so that the response seen is purely due to a tropospheric pathway. Including a more realistic stratosphere would increase complexity, since there likely is a two-way interaction between variability in the stratosphere and ENSO teleconnections (e.g., Ineson and Scaife, 2009; Barriopedro and Calvo, 2014) and is therefore beyond the scope of this study.

In Figure 1c and d, the blocking anomalies for the MJO experiments are shown, which agree remarkably well with results from Henderson *et al.* (2016) and Gollan and Greatbatch (2017). Focusing on the NA and European sector and MJO phase 6 (Figure 1d), there is strongly enhanced MLB frequency over the NA by up to 4%. Over the European continent, positive (negative) MLB anomalies over western (eastern) Europe suggest a westward shift of blocking. For MJO phase 2 (Figure 1c), there is a decrease of MLB over south-eastern Europe and enhanced MLB over north-eastern Europe, suggesting a northward shift of MLB. This northward shift of MLB associated with MJO phase 2 is consistent with the model results of Gollan and Greatbatch (2017), who also find decreased blocking frequency over southern Europe, although this is located further west than in the PUMA results, probably because of the high degree of idealization in the latter. The increase in MLB frequency over western Europe found here for MJO phase 6 is related to a weakened NA storm track and a geopotential height response (see Figure S3), reminiscent of the negative phase of the North Atlantic Oscillation (Greatbatch, 2000; Hurrell *et al.,* 2003), consistent with the observational study by Cassou (2008). The northward shift of MLB for MJO phase 2 is related to negative Z anomalies in the storm track region, acting against the reversal of the gradient of Z related to blocking.

3.2 | MLB bias resulting from a bias in tropical precipitation

In the fifth phase of the Coupled Model Intercomparison Project Phase 5 (CMIP5) models, the aforementioned negative MLB bias over the NA and Europe is still a major issue,

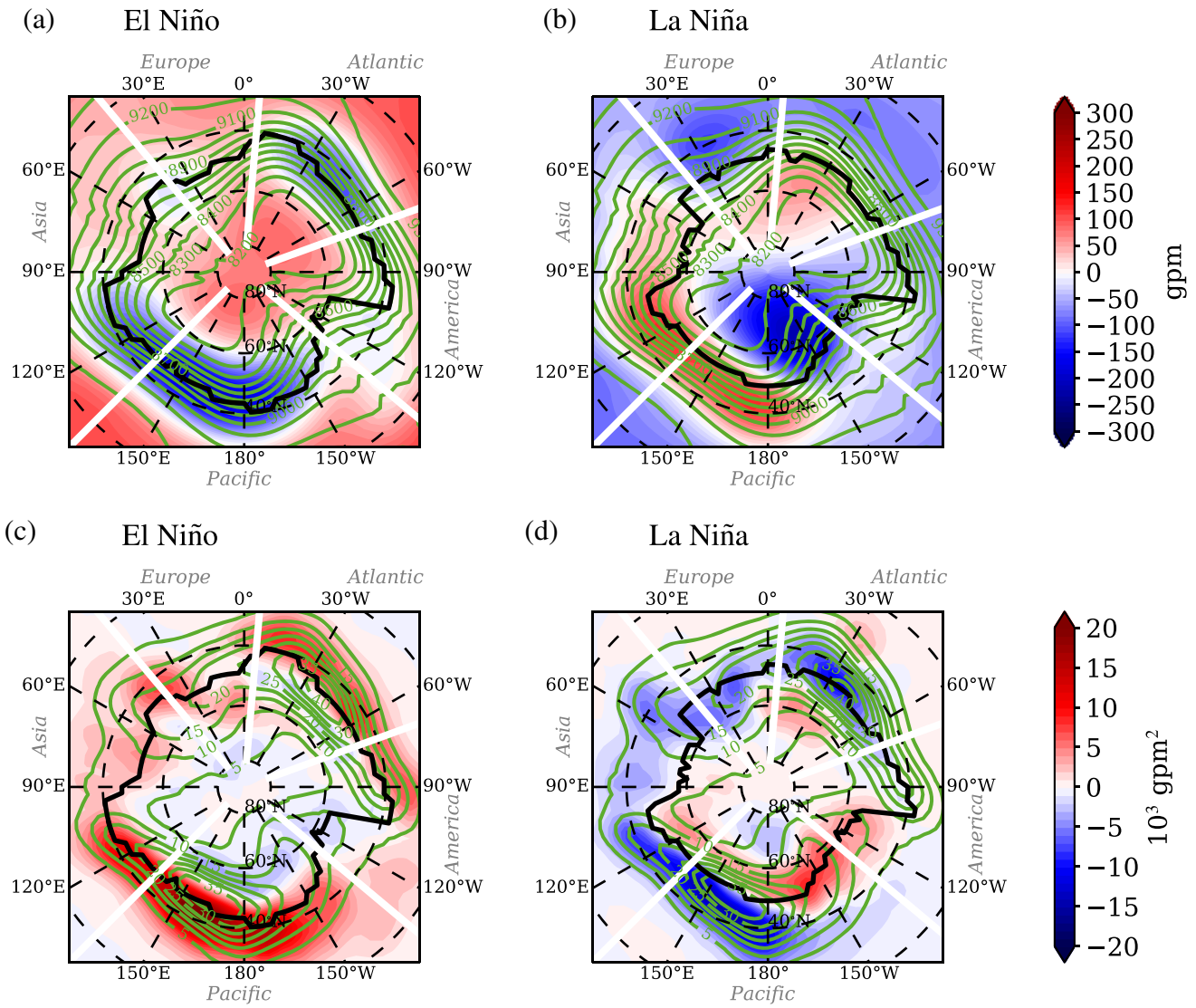

FIGURE 2 Polar stereographic projection of (a, b) *Z* at 300 hPa and (c, d) storm track for (a, c) the El Niño experiment and (b, d) the La Niña experiment. Shading shows anomalies in each case, referring to the climatology of the reference experiment, shown as labeled green contours (contour intervals are 100 gpm for *Z* and 5,000 gpm^2 for the storm track). Black solid contour line indicates the position of the storm track in each experiment. White solid lines separate five different sectors of the Northern Hemisphere, which are indicated on the outside of the boxes (Europe, Atlantic, America, Pacific, and Asia)

see figure 1 in Masato *et al*. (2013). In particular, the "multi-model blocking frequency is less than half of that in ERA-40" over Europe. On the other hand, there is a bias in precipitation in these models, shown as figure 9.4b in Flato *et al*. (2013), dominated by a wet bias in the Tropics, especially near the Indo-Pacific region, and a dry bias over South America. The results from the previous paragraph, concerning ENSO and the MJO, motivated us to test the hypothesis that the bias in precipitation favors the negative bias in MLB. We use a diabatic heating pattern resembling the tropical part of the CMIP5 precipitation bias (see Text S1, Figure S6) and label the corresponding experiment as the CMIP-run. The MLB frequency anomalies and the time mean *Z* anomaly at 300 hPa for the CMIP-run with respect to the reference run are shown in Figure 3a and b. In the NP sector, there is a deepened Aleutian low in the CMIP-run and positive *Z* anomalies in the subtropics leading to an enhanced meridional gradient. Over the NA and European sector, there is also an enhanced meridional gradient in *Z*, mainly due to an increase of *Z* at subtropical latitudes, which is associated with a strengthening of the subtropical jets. The anomalies in *Z* in turn lead to an enhanced storm track (see Figure 3c) showing some southward expansion over the NP, northward expansion over the NA, and eastward expansion over the European continent. Consistent with the stronger meridional Z gradient and the stronger storm tracks, MLB is strongly reduced over most of the Northern Hemisphere midlatitudes. The overall pattern of the anomalies in MLB

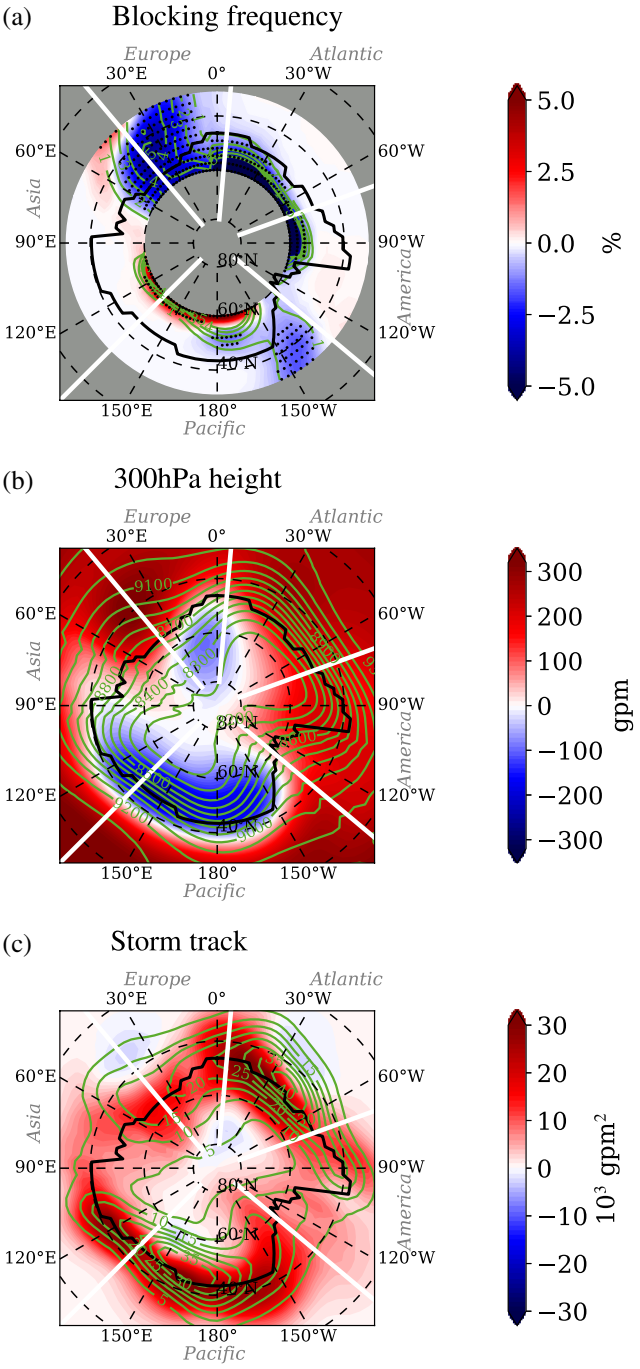

FIGURE 3 Polar stereographic projection of (a) blocking frequency anomaly, (b) *Z* anomaly at 300 hPa, (c) storm track anomaly in the CMIP-run. Black dots in (a) show statistical significance at the 95% level (see supporting information for details). Anomalies of the CMIP-run refer to the climatology of the reference run, shown as labeled green contour lines (contour intervals are 1% for MLB frequency, 100 gpm for *Z* and 5,000 gpm^2 for the storm track). Black solid contour lines in all panels indicate the position of the storm track in the CMIP-run. White solid lines separate five different sectors of the Northern Hemisphere, which are indicated on the outside of the boxes (Europe, Atlantic, America, Pacific, and Asia)

frequency of the CMIP-run is quite similar to the CMIP5 multimodel mean blocking bias, see figure 1 in Masato *et al.* (2013), that is, reduced blocking over central Europe, over the NA and the eastern NP and slightly enhanced blocking over north-eastern Siberia.

4 | SUMMARY AND DISCUSSION

Our results concerning MLB associated with ENSO and the MJO mostly confirm previous studies using reanalysis data and complex models (Barriopedro *et al.,* 2006; Henderson *et al.,* 2016; Gollan and Greatbatch, 2017). In particular, we have shown that in an experiment with El Niño heating there is reduced MLB over the subtropical eastern NP and over eastern Europe and enhanced MLB over the high-latitude NP, western Europe and the NA. In a La Niña-type experiment, we find reduced MLB over the whole NP, but a wide strengthening of MLB over Europe and the NA. Furthermore, for MJO phase 2, we find a northward shift of MLB over Europe and for MJO phase 6 a westward shift of MLB over Europe and a strong enhancement of MLB on the northern flank of the storm track over the NA. Henderson and Maloney (2018) have found a weak decrease of blocking over the high-latitude NA for both phases of ENSO using reanalysis data, while we find an increase of blocking there for both phases of ENSO, both responses being nonlinear. This suggests that the results for blocking over the high-latitude NA are not certain and that the results from our model in that region should be interpreted with caution. The different results compared to reanalysis data (Henderson and Maloney, 2018) could be due to the fact that the end of the Pacific storm track is shifted to the north by about 10° compared to reanalyses, leading to a sharp southward "jump" of the storm track at about 100°W, unlike in reanalyses where the transition between Pacific and Atlantic storm tracks is rather smooth (see Bastin, 2018, figure 3.11). Furthermore, concerning the results on ENSO, the documented response might not exactly be comparable to composites from reanalyses, because here we use as a forcing an idealized monopole heating, whereas in reality ENSO anomalies usually appear as dipole anomalies in diabatic heating of varying relative strengths. Hinton *et al.* (2009) found that the opposing heating centers associated with ENSO can counteract each other with respect to the blocking response over the NP. Therefore, we think using such simplified ENSO heating is an advantage for interpretation.

Using a dry dynamical core model without any stratospheric polar vortex allows us to pin down the MLB response to (a) a purely dynamical process associated with Rossby wave generation, propagation, and breaking and to (b) a purely tropospheric pathway. Concerning (a), the

geopotential height anomalies in the ENSO and MJO experiments suggest a stationary Rossby wave response. As an example, concerning the MJO, one can compare figure S3 and figure 5 in Henderson *et al*. (2016), showing that the stationary Rossby wave response develops after 10 days or more, after which the geopotential height anomalies strongly resemble the results from our simple model. The timescale of 10 days is consistent with Hoskins and Karoly (1981), who used a similar model to investigate the extratropical response to tropical heating. Concerning (b), it is possible that including a more realistic stratosphere in the model would change our results, but the agreement with results from reanalysis suggests that the changes would be minor. That said, the quantitative numbers of percentage changes in MLB presented here should not be taken literally, but rather the qualitative patterns of blocking anomalies.

Our model experiment concerning the CMIP5 model bias in tropical precipitation reproduces the CMIP5 blocking bias, see, for example, figure 1 in Masato *et al*. (2013), particularly well for the NA and European sector and less well for the Pacific sector. Note that there is a larger agreement between previous studies on the blocking bias of CMIP5 models in the NA and European sector than in the Pacific sector, as results for the Pacific are sensitive to the choice of blocking indices and the number of models used for the analysis (see, e.g., Anstey *et al.,* 2013; Davini and D'Andrea, 2016). Our results suggest that the negative MLB bias in most CMIP5 models over the NA and Europe is at least partly caused by the bias in tropical precipitation, that is, the largely too strong tropical precipitation in those models. Thereby, enhanced diabatic tropical heating associated with enhanced precipitation leads to an enhanced poleward temperature gradient in the middle troposphere. The enhanced gradient, due to the thermal wind relation, accelerates the subtropical jet stream, and strengthens the storm tracks, which in turn reduces blocking frequencies at midlatitudes. These results are in agreement with Lu *et al*. (2004), who found an extratropical circulation pattern in response to enhanced heating in the Indo-Pacific region, similar to our results from the CMIP-run. The relation between the two CMIP5 biases—in tropical precipitation and MLB—could serve as a particularly promising possibility to improve the behavior of MLB in complex Earth system models, because tuning tropical precipitation in the models closer to observations could improve MLB climatologies, while tuning is computationally much cheaper than, for example, increasing model resolution.

ACKNOWLEDGEMENTS

We thank the Kiel University Computing Centre for enabling us to perform the experiments presented here. Special thanks go to Prof. Dr. Martin Claus for helping to run PUMA on the Kiel University Computing Centre and to two anonymous reviewers whose comments were helpful when revising the manuscript. We also thank Dr. Tobias Bayr for some helpful discussion on the manuscript. This work was supported by the German Ministry for Education and Research (BMBF) through MiKlip2, subproject 01LP1517D (ATMOS-MODINI). R.J.G. is grateful for continuing support from GEOMAR. Model data necessary to reproduce the figures shown here can be found at https://data.geomar.de.

ORCID

Gereon Gollan https://orcid.org/0000-0002-8329-4168
Swantje Bastin https://orcid.org/0000-0002-5293-5604
Richard J. Greatbatch https://orcid.org/0000-0001-5758-2249

REFERENCES

Anstey, J.A., Davini, P., Gray, L.J., Woollings, T.J., Butchart, N., Cagnazzo, C., Christiansen, B., Hardiman, S.C., Osprey, S.M. and Yang, S. (2013) Multi-model analysis of northern hemisphere winter blocking: model biases and the role of resolution. *Journal of Geophysical Research – Atmospheres*, 118, 3956–3971. https://doi.org/10.1002/jgrd.50231.

Barriopedro, D. and Calvo, N. (2014) On the relationship between ENSO, stratospheric sudden warmings, and blocking. *Journal of Climate*, 27, 4704–4720. https://doi.org/10.1175/JCLI-D-13-00770.1.

Barriopedro, D., García-Herrera, R., Lupo, A.R. and Hernández, E. (2006) A climatology of northern hemisphere blocking. *Journal of Climate*, 19, 1042–1063. https://doi.org/10.1175/JCLI3678.1.

Bastin, S. (2018) *Ingredients for blocking in a dry dynamical atmospheric model.* Master thesis, Kiel University. Available at: http://eprints.uni-kiel.de/44396/ [Accessed 10th April 2019].

Berckmans, J., Woollings, T., Demory, M.E., Vidale, P.L. and Roberts, M. (2013) Atmospheric blocking in a high resolution climate model: influences of mean state, orography and eddy forcing. *Atmospheric Science Letters*, 14, 34–40. https://doi.org/10.1002/asl2.412.

Cassou, C. (2008) Intraseasonal interaction between the Madden-Julian Oscillation and the North Atlantic Oscillation. *Nature*, 455, 523–527. https://doi.org/10.1038/nature07286.

Davini, P. and D'Andrea, F. (2016) Northern hemisphere atmospheric blocking representation in global climate models: twenty years of improvements? *Journal of Climate*, 29, 8823–8840. https://doi.org/10.1175/JCLI-D-16-0242.1.

Flato, G., Marotzke, J., Abiodun, B., Braconnot, P., Chou, S., Collins, W., Cox, P., Driouech, F., Emori, S., Eyring, V., Forest, C., Gleckler, P., Guilyardi, E., Jakob, C., Kattsov, V., Reason, C. and Rummukainen, M. (2013) Evaluation of climate models. In: Stocker, T.F., Qin, D., Plattner, G.-K., Tignor, M., Allen, S.K., Boschung, J., Nauels, A., Xia, Y., Bex, V. and Midgley, P. (Eds.) *Climate Change 2013: The Physical Science Basis. Contribution of Working Group I to the Fifth Assessment Report of the Intergovernmental Panel on Climate Change.*

Cambridge: Cambridge University Press, pp. 760–766. https://doi.org/10.1017/CBO9781107415324.020.

Fraedrich, K., Kirk, E. and Lunkeit, F. (1998) *PUMA: Portable University model of the atmosphere.* Technical report, DKRZ. https://doi.org/10.2312/WDCC/DKRZ_Report_No16.

Franzke, C., Fraedrich, K. and Lunkeit, F. (2000) Low-frequency variability in a simplified atmospheric global circulation model: storm-track induced spatial resonance. *Quarterly Journal of the Royal Meteorological Society*, 126, 2691–2708. https://doi.org/10.1002/qj.49712656905.

Gollan, G. and Greatbatch, R.J. (2017) The relationship between northern hemisphere winter blocking and tropical modes of variability. *Journal of Climate*, 30, 9321–9337. https://doi.org/10.1175/JCLI-D-16-0742.1.

Gollan, G., Greatbatch, R.J. and Jung, T. (2015) Origin of variability in northern hemisphere winter blocking on interannual to decadal time scales. *Geophysical Research Letters*, 42, 10,037–10,046. https://doi.org/10.1002/2015GL066572.

Greatbatch, R.J. (2000) The North Atlantic Oscillation. *Stochastic Environmental Research and Risk Assessment*, 14, 213–242. https://doi.org/10.1007/s004770000047.

Held, I.M. and Suarez, M.J. (1994) A proposal for the intercomparison of the dynamical cores of atmospheric general circulation models. *Bulletin of the American Meteorological Society*, 75, 1825–1830. https://doi.org/10.1175/1520-0477(1994)075<1825:APFTIO>2.0.CO;2.

Henderson, S.A. and Maloney, E.D. (2018) The impact of the Madden-Julian oscillation on high-latitude winter blocking during El Niño-Southern Oscillation events. *Journal of Climate*, 31, 5293–5318. https://doi.org/10.1175/JCLI-D-17-0721.1.

Henderson, S.A., Maloney, E.D. and Barnes, E.A. (2016) The influence of the Madden-Julian Oscillation on northern hemisphere winter blocking. *Journal of Climate*, 29, 4597–4616. https://doi.org/10.1175/JCLI-D-15-0502.1.

Hinton, T.J., Hoskins, B.J. and Martin, G.M. (2009) The influence of tropical sea surface temperatures and precipitation on North Pacific atmospheric blocking. *Climate Dynamics*, 33, 549–563. https://doi.org/10.1007/s00382-009-0542-7.

Hoskins, B.J. and Karoly, D.J. (1981) The steady linear response of a spherical atmosphere to thermal and orographic forcing. *Journal of the Atmospheric Sciences*, 38, 1179–1196. https://doi.org/10.1175/1520-0469(1981)038<1179:TSLROA>2.0.CO;2.

Hoskins, B.J. and Simmons, A.J. (1975) A multi-layer spectral model and the semi-implicit method. *Quarterly Journal of the Royal Meteorological Society*, 101, 637–655. https://doi.org/10.1002/qj.49710142918.

Hurrell, J.W., Kushnir, Y., Ottersen, G. and Visbeck, M. (2003) An overview of the North Atlantic oscillation. *American Geophysical Union. Geophysical Monograph*, 134, 1–36. https://doi.org/10.1029/134GM01.

Ineson, S. and Scaife, A.A. (2009) The role of the stratosphere in the European climate response to El Niño. *Nature Geoscience*, 2, 32–36. https://doi.org/10.1038/ngeo381.

Jung, T., Balsamo, G., Bechtold, P., Beljaars, A.C.M., Köhler, M., Miller, M.J., Morcrette, J.-J., Orr, A., Rodwell, M.J. and Tompkins, A.M. (2010) The ECMWF model climate: recent progress through improved physical parametrizations. *Quarterly Journal of the Royal Meteorological Society*, 136, 1145–1160. https://doi.org/10.1002/qj.634.

Jung, T., Miller, M.J., Palmer, T.N., Towers, P., Wedi, N., Achuthavarier, D., Adams, J.M., Altshuler, E.L., Cash, B.A., Kinter, J.L., Marx, L., Stan, C. and Hodges, K.I. (2012) High-resolution global climate simulations with the ECMWF model in project Athena: experimental design, model climate, and seasonal forecast skill. *Journal of Climate*, 25, 3155–3172. https://doi.org/10.1175/JCLI-D-11-00265.1.

Lu, J., Greatbatch, R.J. and Peterson, K.A. (2004) Trend in northern hemisphere winter atmospheric circulation during the last half of the twentieth century. *Journal of Climate*, 17, 3745–3760. https://doi.org/10.1175/1520-0442(2004)017<3745:TINHWA>2.0.CO;2.

Masato, G., Hoskins, B.J. and Woollings, T. (2013) Winter and summer northern hemisphere blocking in CMIP5 models. *Journal of Climate*, 26, 7044–7059. https://doi.org/10.1175/JCLI-D-12-00466.1.

Morita, J., Takayabu, Y.N., Shige, S. and Kodama, Y. (2006) Analysis of rainfall characteristics of the Madden-Julian oscillation using TRMM satellite data. *Dynamics of Atmospheres and Oceans*, 42, 107–126. https://doi.org/10.1016/j.dynatmoce.2006.02.002.

Renwick, J.A. and Wallace, J.M. (1996) Relationships between North Pacific wintertime blocking, El Niño, and the PNA pattern. *Monthly Weather Review*, 124, 2071–2076. https://doi.org/10.1175/1520-0493(1996)124<2071:RBNPWB>2.0.CO;2.

Sardeshmukh, P.D. and Hoskins, B.J. (1988) The generation of global rotational flow by steady idealized tropical divergence. *Journal of the Atmospheric Sciences*, 45, 1228–1251. https://doi.org/10.1175/1520-0469(1988)045<1228:TGOGRF>2.0.CO;2.

Scaife, A.A., Copsey, D., Gordon, C., Harris, C., Hinton, T.J., Keeley, S.P.E., O'Neill, A., Roberts, M.J. and Williams, K.D. (2011) Improved Atlantic winter blocking in a climate model. *Geophysical Research Letters*, 38, 1–6. https://doi.org/10.1029/2011GL049573.

Scherrer, S.C., Croci-Maspoli, M., Schwierz, C. and Appenzeller, C. (2006) Two-dimensional indices of atmospheric blocking and their statistical relationship with winter climate patterns in the Euro-Atlantic region. *International Journal of Climatology*, 26, 233–249. https://doi.org/10.1002/joc.1250.

Wheeler, M.C. and Hendon, H.H. (2004) An all-season real-time multivariate MJO index: development of an index for monitoring and prediction. *Monthly Weather Review*, 132, 1917–1932. https://doi.org/10.1175/1520-0493(2004)132<1917:AARMMI>2.0.CO;2.

Woollings, T., Charlton-Perez, A., Ineson, S., Marshall, A.G. and Masato, G. (2010) Associations between stratospheric variability and tropospheric blocking. *Journal of Geophysical Research*, 115, D06108. https://doi.org/10.1029/2009JD012742.

SUPPORTING INFORMATION

Additional supporting information may be found online in the Supporting Information section at the end of this article.

How to cite this article: Gollan G, Bastin S, Greatbatch RJ. Tropical precipitation influencing boreal winter midlatitude blocking. *Atmos Sci Lett*. 2019;20:e900. https://doi.org/10.1002/asl.900